Magnetic phase transitions in narrow nondegenerate energy bands

S. Bei der Kellen, W. Nolting, and G. Borstel
Universität Osnabrück, Fachbereich Physik, Barbarastrasse 7, D-4500 Osnabrück, Federal Republic of Germany
(Received 20 December 1989)

By use of an effective-medium approach for an approximate but self-consistent solution of the s-band Hubbard model, the possibility and stability of spontaneous magnetic order in narrow energy bands are investigated for arbitrary band occupation ($0 \leq n \leq 2$) and arbitrary Coulomb coupling U/W. The starting point is a solid with rocksalt structure and a MnO-type sublattice decomposition. Ferromagnetic as well as antiferromagnetic solutions appear for more than half-filled bands ($n > 1$). Antiferromagnetism is stable in a small stripe close above $n = 1$. The corresponding phase diagram is derived and discussed. The critical temperatures T_C, T_N are strongly (n, U)-dependent, but in any case of realistic order of magnitude. A detailed physical interpretation of the results is offered by inspecting the temperature behavior of the quasiparticle density of states. Higher expectation values like $\langle c_{i-\sigma}^{\dagger} c_{j-\sigma} n_{i\sigma} \rangle$ turn out to be the decisive preconditions for spontaneous band magnetism.

I. INTRODUCTION

The possibility of spontaneous magnetic ordering due to strong electron correlations in narrow energy bands is commonly investigated within the framework of the Hubbard model.[1-3] In spite of the simple structure of the model Hamiltonian, the general solution of the underlying many-body problem is not available. Rigorous results exist only for very few cases, concerning the one-dimensional model,[4,5] clusters of finite size,[6,7] the ($T=0$, $U \rightarrow \infty$) case for special particle numbers $N_e = N \pm 1$ (Ref. 8) [$N(N_e)$: number of lattice sites (band electrons), U: intra-atomic Coulomb interaction], the atomic limit $W=0$ (W: width of the free Bloch band), and the trivial limit $U=0$. These special cases are of great importance for testing unavoidable approximate procedures for the general problem, yielding, however, only restricted information about the magnetic properties of highly correlated electron systems. Although the fundamental question, whether or not the simple s-band Hubbard model may exhibit band magnetism, is not yet assured rigorously, many convincing approximate theories predict the existence of collective magnetism under certain conditions for the basic model parameters. The decisive terms are obviously the Coulomb correlation U/W, the temperature T, the band occupation $n = N_e/N$ ($0 \leq n \leq 2$, s band), and the lattice structure. The main goal for a topical study must therefore be the derivation of magnetic phase diagrams in dependence of these parameters.

No controversy exists about very weakly occupied energy bands ($n \ll 1$), for which no collective magnetic order will appear irrespective of the value of the Coulomb coupling U.[9] On the other hand, the intensively studied half-filled band ($n = 1$) should have an antiferromagnetic ground state.[10] But, what happens for partially filled ($0 < n < 1$; $1 < n < 2$) bands? Recently, a self-consistent spectral density approach (SDA) has been used[11] to compare the stability of paramagnetic, ferromagnetic, and antiferromagnetic solutions of the Hubbard model. The starting point was a simple symmetric model density of states being thought to simulate a lattice which consists of two interpenetrating sublattices A and B. The main results may be gathered as follows: Antiferromagnetism is stable in a restricted region of n around the half-filled band, which is broadest for intermediate coupling strengths ($U/W \approx 1$), and shrinks to the $n=1$ axis for $U/W \rightarrow \infty$ and $U/W \rightarrow 0+$. For smaller n, which, however, have to exceed a critical value, and for couplings U/W, being greater than a minimum value, ferromagnetism becomes stable, while for very low band occupations the system is paramagnetic irrespective of U. The phase diagram is symmetric to the $n=1$ axis because of particle-hole symmetry. The calculated critical temperatures are of realistic order of magnitude.[11]

We think that the theory of Ref. 11 has left behind some challenging questions, concerning, e.g., the influence of the lattice structure on the magnetic state. There is some evidence that the results of Ref. 11 will substantially modify, if one uses, e.g., a nonsymmetric Bloch density of states (BDOS), excluding therewith particle-hole symmetry. In particular for antiferromagnetic systems we have to expect a remarkable structure dependence. The quasiparticle density of states (QDOS), derived in Ref. 11 for an antiferromagnetic solid, is characterized by two energy gaps. One is the so-called Hubbard gap, which appears for strong enough couplings U/W in para- and ferromagnetic systems, too, being a typical consequence of the electron correlations. The other gap is due to the antiferromagnetic ordering giving rise to a reduced magnetic Brillouin zone. This so-called Slater gap opens for all temperatures below T_N, at least for model densities of states like that used in Ref. 11. For the special case $T=0$ it has also been found for more realistic systems, its existence being, however, strongly dependent on details of the antiferromagnetic ordering.[12,13]

In this paper we want to derive the magnetic phase diagram for a correlated electron system on a lattice with a realistic rocksalt structure. One aim is to demonstrate in comparison with the results of Ref. 11 the strong structure dependence of the magnetic properties of the Hubbard model. We compare paramagnetic, ferromagnetic, and antiferromagnetic spin structures, assuming that neighboring (111) planes of the fcc lattice belong to different sublattices A and B. In the case of antiferromagnetism each sublattice orders ferromagnetically, but with an alternating *NSNS* magnetization sequence (MnO-type antiferromagnetism). In particular, we shall expect consequences of the asymmetry of the free Bloch density of states (BDOS) which prevents particle-hole symmetry. For an approximate solution of the underlying many-body problem an effective-medium approach is used, which for para- and ferromagnetism turns out to be equivalent to the SDA,[11] being, however, very much simpler in the case of antiferromagnetic spin structures.

Besides the magnetic phase diagram the most weighty criteria for the trustworthiness of a theoretical approach to band magnetism are the transition temperatures T_C and T_N, respectively. The success of the SDA procedure[11] lies mainly in yielding realistic $T_{C,N}$ values, contrary to the frequently applied Stoner model. The multiband SDA (Ref. 14) resulted in an excellent description of magnetic and spectroscopic data of the prominent band ferromagnet Ni.[14–16]. In the same spirit it belongs to the most important intentions of this work to provide the basis for a forthcoming study on the antiferromagnetic Mott-Hubbard insulator NiO. For this purpose we need a many-body approach, which fulfills two conditions. It must be, on the one hand, mathematically on a tractable level, i.e., simple enough, but, on the other hand, also realistic enough, to promise a quantitative description of NiO when combined with a reliable one-electron band structure calculation for the BDOS. The SDA of Ref. 11 appears to be too complicated to be successfully applied to antiferromagnetic systems like NiO.

II. MODEL

Strongly correlated electrons in narrow, nondegenerate energy bands are usually studied within the framework of the well-known Hubbard model.[1–3] Since we intend to study simultaneously the possibility of paramagnetism, ferromagnetism, and antiferromagnetism, we presume a lattice, which can be decomposed into two chemically equivalent sublattices A and B. We refer to the total lattice as a "magnetic" Bravais lattice ($\mathbf{R}_i$) with a two-atom basis ($\mathbf{r}_\alpha$). The space vector of any lattice site is then given by

$$\mathbf{R}_{i\alpha}=\mathbf{R}_i+\mathbf{R}_\alpha \quad (i=1,\ldots,N)\ (\alpha=A,B)\ . \tag{1}$$

N denotes the number of sites in the magnetic Bravais lattice. $2N$ is then the total number of sites in the real, chemical lattice. Translational symmetry can be assumed for the magnetic structure. The thermodynamical average of any site-dependent operator $O_{i\alpha}$,

$$\langle O_{i\alpha}\rangle \equiv \langle O_\alpha\rangle\ , \tag{2}$$

is surely $\mathbf{R}_i$ independent. A dependence on the sublattice index α, however, may happen, in particular in antiferromagnetic phases. Fourier transformations between real space and $\mathbf{k}$ space are therefore restricted to the magnetic lattice and the magnetic Brillouin zone, respectively:

$$O_{i\alpha}=\frac{1}{\sqrt{N}}\sum_{\mathbf{k}} e^{i\mathbf{k}\cdot\mathbf{R}_i}O_{\mathbf{k}\alpha}\ , \tag{3}$$

$$O_{\mathbf{k}\alpha}=\frac{1}{\sqrt{N}}\sum_{i=1}^{N} e^{-i\mathbf{k}\cdot\mathbf{R}_i}O_{i\alpha}\ . \tag{4}$$

Taking into account the sublattice structure the Hamiltonian of the Hubbard model reads

$$\mathcal{H}=\sum_{i,j,\sigma,\alpha,\beta}(T_{ij}^{\alpha\beta}-\mu\delta_{ij}\delta_{\alpha\beta})c_{i\alpha\sigma}^{\dagger}c_{j\beta\sigma}+\frac{U}{2}\sum_{i,\alpha,\sigma} n_{i\alpha\sigma}n_{i\alpha-\sigma}\ . \tag{5}$$

$c_{i\alpha\sigma}^{\dagger}$ ($c_{i\alpha\sigma}$) is the creation (annihilation) operator of an electron with spin σ at site $\mathbf{R}_{i\alpha}$. $n_{i\alpha\sigma}=c_{i\alpha\sigma}^{\dagger}c_{i\alpha\sigma}$ is the number operator, μ the chemical potential, U the intraatomic Coulomb-matrix element, and $T_{ij}^{\alpha\beta}$ the hopping integral between sites $\mathbf{R}_{i\alpha}$ and $\mathbf{R}_{j\beta}$. The latter express the kinetic energy of the band electrons and the influence of the periodic lattice potential. In a tight-binding approximation we restrict the electron hopping to nearest neighbors ($\Delta_1^{\alpha\beta}$) in the chemical lattice:

$$T_{ij}^{\alpha\beta}=\begin{cases}T_0, & \text{if } \mathbf{R}_{i\alpha}=\mathbf{R}_{j\beta}\\ T_1, & \text{if } \mathbf{R}_{i\alpha}=\mathbf{R}_{j\beta}+\Delta_1^{\alpha\beta}\\ 0, & \text{otherwise}\ .\end{cases} \tag{6}$$

In the single-band case we can choose for simplicity $T_0=0$. For the $\mathbf{k}$-dependent Bloch energies

$$\varepsilon_{\alpha\beta}(\mathbf{k})=\sum_{i,j} T_{ij}^{\alpha\beta}e^{-i\mathbf{k}\cdot(\mathbf{R}_i-\mathbf{R}_j)}\ , \tag{7}$$

one finds with (6)

$$\varepsilon(\mathbf{k})\equiv\varepsilon_{AA}(\mathbf{k})=\varepsilon_{BB}(\mathbf{k})=T_0+T_1f(\mathbf{k})\ , \tag{8}$$

$$t(\mathbf{k})\equiv\varepsilon_{AB}(\mathbf{k})=\varepsilon_{BA}^{*}(\mathbf{k})=T_1g(\mathbf{k})\ . \tag{9}$$

$f(\mathbf{k})$ and $g(\mathbf{k})$ are determined by the lattice structure:

$$f(\mathbf{k})=\sum_{\Delta_1^{AA}} e^{-i\mathbf{k}\cdot\Delta_1^{AA}}\ ,\qquad g(\mathbf{k})=\sum_{\Delta_1^{AB}} e^{-i\mathbf{k}\cdot\Delta_1^{AB}}\ . \tag{10}$$

We consider a fcc structure with lattice constant a. The (111) planes belong in an alternating sequence to sublattice A and sublattice B, respectively. Each atom has twelve nearest neighbors, six from the same and six from the other sublattice:

$$f(\mathbf{k})=2\left[\cos\left[\frac{a}{2}(k_x-k_y)\right]+\cos\left[\frac{a}{2}(k_y-k_z)\right]+\cos\left[\frac{a}{2}(k_z-k_x)\right]\right], \tag{11}$$

$$g(\mathbf{k})=2\left[\cos\left[\frac{a}{2}(k_x+k_y)\right]+\cos\left[\frac{a}{2}(k_y+k_z)\right]+\cos\left[\frac{a}{2}(k_z+k_x)\right]\right]. \tag{12}$$

T_1 is closely related to the width W of the Bloch band:

$$W=-16T_1 . \tag{13}$$

The band structure and the total Bloch density of states (BDOS) $\rho_0(E)$ for the noninteracting electron system,

$$\rho_0(E)=\frac{1}{2N}\sum_{\mathbf{k}}\sum_{p=\pm}\delta(E-\varepsilon(\mathbf{k})-p|t(\mathbf{k})|) , \tag{14}$$

are plotted in Fig. 1. We stress once more that the $\mathbf{k}$ summation runs over the first Brillouin zone of the magnetic lattice. In the case of the free system the decomposition into sublattices is of course meaningless. $\rho_0(E)$ is therefore nothing else than the well-known fcc-tight-binding BDOS.

The main goal of our study concerns the relative stability of paramagnetism, ferromagnetism, and antiferromagnetism in a solid with the previously described structure. We investigate this question in terms of temperature T, Coulomb interaction U, and band occupation n $(0\le n\le 2)$. A key quantity will be the sublattice magnetization

$$m_A=\langle n_{A\uparrow}\rangle-\langle n_{A\downarrow}\rangle\equiv m . \tag{15}$$

Since we assume each sublattice to be either para- or ferromagnetic, it holds,

$$m_A=m_B \tag{16}$$

for a para- or ferromagnet, and

$$m_A=-m_B \tag{17}$$

for an antiferromagnet. The sublattice-magnetization is determined by the spin-dependent average particle numbers

$$\langle n_{\alpha\sigma}\rangle=\frac{1}{\hbar}\int_{-\infty}^{+\infty}dE\, f_-(E)S_{ii\sigma}^{\alpha\alpha}(E-\mu) , \tag{18}$$

$$f_-(E)=\frac{1}{e^{\beta(E-\mu)}+1} , \tag{19}$$

which can be derived from the one-electron spectral density:

$$S_{ij\sigma}^{\alpha\beta}(E)=\int_{-\infty}^{+\infty}d(t-t')e^{(i/\hbar)E(t-t')}\frac{1}{2\pi}\times\langle[c_{i\alpha\sigma}(t),c_{j\beta\sigma}^{\dagger}(t')]_+\rangle . \tag{20}$$

$[\ldots,\ldots]_+$ denotes the anticommutator. The knowledge of $S_{\mathbf{k}\sigma}^{\alpha\beta}(E)$ as its $\mathbf{k}$-dependent Fourier transform,

$$S_{\mathbf{k}\sigma}^{\alpha\beta}(E)=\frac{1}{N}\sum_{i,j}S_{ij\sigma}^{\alpha\beta}(E)e^{-i\mathbf{k}\cdot(\mathbf{R}_i-\mathbf{R}_j)} , \tag{21}$$

solves the full problem. Closely related to this function is the quasiparticle density of states (QDOS),

$$\rho_\sigma(E)=\frac{1}{2\hbar}\sum_{\alpha}S_{ii\sigma}^{\alpha\alpha}(E-\mu)=\frac{1}{2N\hbar}\sum_{\alpha}\sum_{\mathbf{k}}S_{\mathbf{k}\sigma}^{\alpha\alpha}(E-\mu) , \tag{22}$$

which is thought of being built up by the two sublattice QDOS $\rho_{\alpha\sigma}(E)$:

$$\rho_{\alpha\sigma}(E)=\frac{1}{N\hbar}\sum_{\mathbf{k}}S_{\mathbf{k}\sigma}^{\alpha\alpha}(E-\mu) . \tag{23}$$

For para- and ferromagnetic systems $\rho_\sigma(E)$ and $\rho_{\alpha\sigma}(E)$ are of course identical, while for antiferromagnets the relation $\rho_{A\sigma}(E)=\rho_{B-\sigma}(E)$ holds. Sometimes it may be convenient to start the calculation with the retarded one-electron Green function,

$$G_{ij\sigma}^{\alpha\beta}(t,t')\equiv\langle\langle c_{i\alpha\sigma}(t);c_{j\beta\sigma}^{\dagger}(t')\rangle\rangle\equiv-i\Theta(t-t')\langle[c_{i\alpha\sigma}(t),c_{j\beta\sigma}^{\dagger}(t')]_+\rangle \tag{24}$$

$[\Theta(t-t')$ is the step function], the imaginary part of which is directly connected to the spectral density:

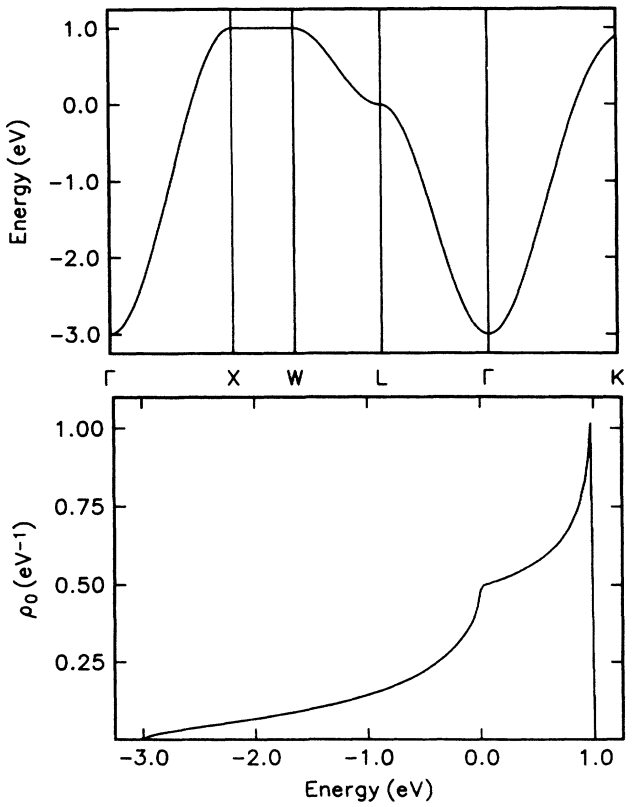

FIG. 1. Tight-binding Bloch band structure and density of states $\rho_0(E)$ for the fcc lattice.

$$S_{ij\sigma}^{\alpha\beta}(E)=-\frac{1}{\pi}\mathrm{Im}[G_{ij\sigma}^{\alpha\beta}(E+i0^+)] . \tag{25}$$

The fundamental spectral density is not exactly derivable for the general Hubbard model. Approximations must be tolerated. Our proposal is exposed in the next section.

III. EFFECTIVE-MEDIUM APPROACH

By use of the commutator

$$[c_{i\alpha\sigma},\mathcal{H}]_-=\sum_{m,\gamma}(T_{im}^{\alpha\gamma}-\mu\delta_{im}\delta_{\alpha\gamma})c_{m\gamma\sigma}+Un_{i\alpha-\sigma}c_{i\alpha\sigma} , \tag{26}$$

we get the equation of motion of the energy-dependent one-electron Green function $G_{ij\sigma}^{\alpha\beta}(E)$:

$$\sum_{m,\gamma}[(E+\mu)\delta_{im}\delta_{\alpha\gamma}-T_{im}^{\alpha\gamma}]G_{mj\sigma}^{\gamma\beta}(E)=\hbar\delta_{ij}\delta_{\alpha\beta}+U\Gamma_{iii;j\sigma}^{\alpha\alpha\alpha;\beta}(E) . \tag{27}$$

On the right-hand side appears the higher Green function

$$\Gamma_{imn;j\sigma}^{\alpha\gamma\delta;\beta}(E)=\langle\langle c_{i\alpha-\sigma}^{\dagger}c_{m\gamma-\sigma}c_{n\delta\sigma};c_{j\beta\sigma}^{\dagger}\rangle\rangle_E , \tag{28}$$

which prevents a direct solution of the problem. If we define via

$$U\Gamma_{iii;j\sigma}^{\alpha\alpha\alpha;\beta}(E)\equiv\sum_{m,\gamma}M_{im\sigma}^{\alpha\gamma}(E)G_{mj\sigma}^{\gamma\beta}(E) \tag{29}$$

the electronic self-energy $M_{ij\sigma}^{\alpha\beta}(E)$, then the formal solution of (27) is easily found:

$$\hat{G}_{\mathbf{k}\sigma}(E)=\frac{\hbar}{\Delta_{\mathbf{k}\sigma}(E)}\begin{bmatrix}E+\mu-\varepsilon(\mathbf{k})-M_{\mathbf{k}\sigma}^{BB}(E) & t(\mathbf{k})+M_{\mathbf{k}\sigma}^{AB}(E)\\ t^*(\mathbf{k})+M_{\mathbf{k}\sigma}^{BA}(E) & E+\mu-\varepsilon(\mathbf{k})-M_{\mathbf{k}\sigma}^{AA}(E)\end{bmatrix} . \tag{30}$$

Here we have written for abbreviation

$$\Delta_{\mathbf{k}\sigma}(E)=[E-R_\sigma^{(+)}(\mathbf{k},E)][E-R_\sigma^{(-)}(\mathbf{k},E)] , \tag{31}$$

$$R_\sigma^{(\pm)}(\mathbf{k},E)=\varepsilon(\mathbf{k})+\tfrac{1}{2}[M_{\mathbf{k}\sigma}^{AA}(E)+M_{\mathbf{k}\sigma}^{BB}(E)]\pm\{\tfrac{1}{4}[M_{\mathbf{k}\sigma}^{AA}(E)-M_{\mathbf{k}\sigma}^{BB}(E)]^2+|t(\mathbf{k})+M_{\mathbf{k}\sigma}^{AB}(E)|^2\}^{1/2} . \tag{32}$$

The remaining problem rests on an approximate derivation of the electronic self-energy. The idea of our approach may be sketched as follows. First we suppress the off-diagonal part $M_{\mathbf{k}\sigma}^{AB}(E)$ of the self-energy, which surely plays only a minor role with respect to the possibility of band magnetism. In the case of para- and ferromagnetism this quantity is even exactly zero. For antiferromagnetic systems it is effectively spin independent and of certainly less importance than the decisive sublattice self-energies $M_{\mathbf{k}\sigma}^{AA}(E)$ and $M_{\mathbf{k}\sigma}^{BB}(E)$. For an explicit determination of these self-energy parts we switch off for the moment the intersublattice hopping $t(\mathbf{k})$ in the model Hamiltonian (5), in order to avoid a double counting of such a term, which enters explicitly the formal solution (30)–(32). That means, in a sense we treat the two ferromagnetic sublattices separately, by applying to the rest Hamiltonian the moment-equating spectral density approach (SDA) of Ref. 11. Proceeding strictly along the line exposed in Ref. 11, one finally gets

$$M_\sigma^{\alpha\alpha}(E)\equiv M_{\mathbf{k}\sigma}^{\alpha\alpha}(E)=U\langle n_{\alpha-\sigma}\rangle\frac{E+\mu-B_{\alpha-\sigma}}{E+\mu-B_{\alpha-\sigma}-U(1-\langle n_{\alpha-\sigma}\rangle)} . \tag{33}$$

This expression contains two important expectation values, the average spin-dependent particle numbers $\langle n_{\alpha-\sigma}\rangle$, and, most decisively, the spin dependent band shift $B_{\alpha-\sigma}$. The latter is composed of higher correlations, which turn out to be necessary for the appearance of a spontaneous spin ordering in the partially filled energy band:

$$\langle n_{\alpha-\sigma}\rangle(1-\langle n_{\alpha-\sigma}\rangle)B_{\alpha-\sigma}=\frac{1}{N}\sum_{i,j,\beta}T_{ij}^{\alpha\beta}\langle c_{i\alpha-\sigma}^{\dagger}c_{j\beta-\sigma}(2n_{i\alpha\sigma}-1)\rangle . \tag{34}$$

The crucial point of our procedure is that the expectation values $\langle n_{\alpha-\sigma}\rangle$ and $B_{\alpha-\sigma}$ are to be determined self-consistently within the *full* model (5). This is possible, since the band shift $B_{\alpha-\sigma}$, although consisting of higher correlation functions, is nevertheless expressable by the one-electron spectral density only. Using Eqs. (3.30) and (3.31) of Ref. 11 expression (34) may be rewritten as:

$$\langle n_{\alpha-\sigma}\rangle(1-\langle n_{\alpha-\sigma}\rangle)B_{\alpha-\sigma}=\frac{1}{N\hbar}\sum_{\mathbf{k}}\sum_{\beta,\gamma}\varepsilon_{\alpha\beta}(\mathbf{k})h_{\mathbf{k}-\sigma}^{\alpha\beta\gamma} , \tag{35}$$

where

$$h_{\mathbf{k}-\sigma}^{\alpha\beta\gamma}\equiv\int_{-\infty}^{+\infty}dE\,f_-(E)\left[\frac{2}{U}[E\delta_{\gamma\alpha}-\varepsilon_{\gamma\alpha}(\mathbf{k})]-\delta_{\gamma\alpha}\right]\times S_{\mathbf{k}-\sigma}^{\beta\gamma}(E-\mu) . \tag{36}$$

Equations (18)–(21), (24), (25), and (30)–(36) build a closed system of equations, which can be solved self-

consistently for the average occupation numbers $\langle n_{\alpha\uparrow}\rangle, \langle n_{\alpha\downarrow}\rangle$.

Under certain conditions there may exist more than one mathematical solution of our closed system of equations. Then the internal energy $E_0(T)$,

$$E_0(T)=\frac{\langle H\rangle}{N}=\frac{1}{N}\sum_{i,\alpha,j,\beta,\sigma} T_{ij}^{\alpha\beta}\langle c_{i\alpha\sigma}^{\dagger}c_{j\beta\sigma}\rangle + \frac{U}{2}\sum_{i,\alpha,\sigma}\langle n_{i\alpha\sigma}n_{i\alpha-\sigma}\rangle , \tag{37}$$

or better the free energy $F(T)$,

$$F(T)=E_0(0)-T\int_0^T \frac{dT'}{T'^2}[E_0(T')-E_0(0)] , \tag{38}$$

may be used to sort out the physically stable solution. The first expectaion value in (37) follows directly via the spectral theorem from the one-electron spectral density $S_{ij\sigma}^{\alpha\beta}(E)$. The second expectation value $\langle n_{i\alpha\sigma}n_{i\alpha-\sigma}\rangle$ is obviously a special case of the higher correlation function needed in (34). Therefore we can take it as a by-product of the transition from (34) to (36):

$$E_0(T)=\frac{1}{2N\hbar}\sum_{\mathbf{k}}\sum_{\sigma,\alpha,\beta}\int_{-\infty}^{+\infty} dE\, f_-(E)[E\delta_{\alpha\beta}+\varepsilon_{\alpha\beta}(\mathbf{k})] \times S_{\mathbf{k}\sigma}^{\beta\alpha}(E-\mu) . \tag{39}$$

We stress once more that the relations between the fundamental spectral density and the average particle numbers (18), the spin-dependent band shift (35) and (36), and the thermodynamic potentials (38) and (39) are rigorous expressions. The unavoidable approximation within our procedure concerns excludingly the self-energy ansatz (33). The self-consistent procedure, proposed previously, will certainly remove a great portion of the insufficiencies being due to (33).

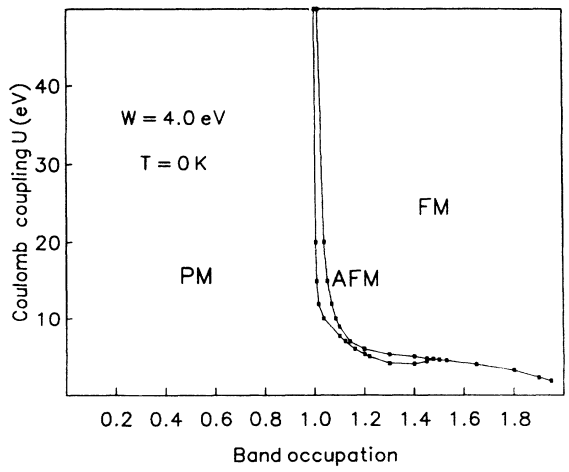

FIG. 2. Phase diagram for $T=0$. The lines indicate the phase boundaries between the paramagnetic (PM), ferromagnetic (FM), and antiferromagnetic (AFM) phase.

IV. RESULTS

The main parameters of the Hubbard model are the coupling constant U/W, the band occupation n, the temperature T, and, last but not least, the lattice structure. For the lattice we have chosen a realistic fcc structure with a sublattice decomposition as described in Sec. II. It should be pointed out that all wave-vector summations have been done explicitly over the first Brillouin zone of the magnetic Bravais lattice without further simplifications. The Bloch bandwidth W has been fixed at 4 eV, so that the final results of our theory appear in terms of U, T, and n.

Figure 2 shows the $T=0$ magnetic phase diagram in dependence of U and n. For a less than half-filled band ($n<1$) we do not find any solution with nonzero magnetization m. This changes for band fillings $n>1$. In wide regions of the phase diagram additional ferromagnetic and antiferromagnetic solutions appear besides the ever-existing paramagnetic one. Equation (39) for the internal

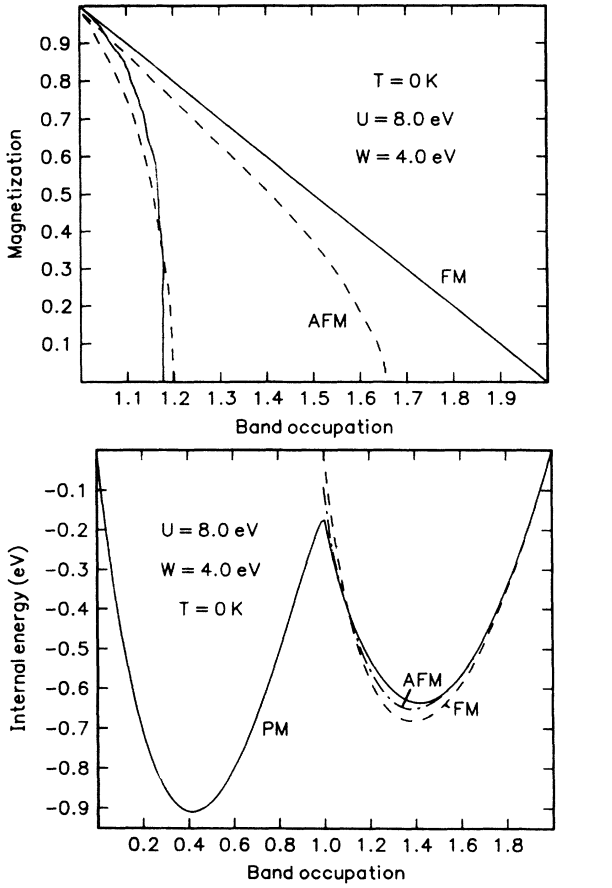

FIG. 3. Upper part: (Sublattice) magnetization m as function of band occupation n for $T=0$. Solid lines indicate the magnetization of the ferromagnetic solutions, while dashed lines belong to the antiferromagnetic solutions. Lower part: Internal energy E_0 as a function of band occupation n for $T=0$. For $n>1$ the values plotted are $E_0-2U(n-1)$. Solid line: paramagnetic solution, dashed line: ferromagnetic solution, dashed-dotted line: antiferromagnetic solution.

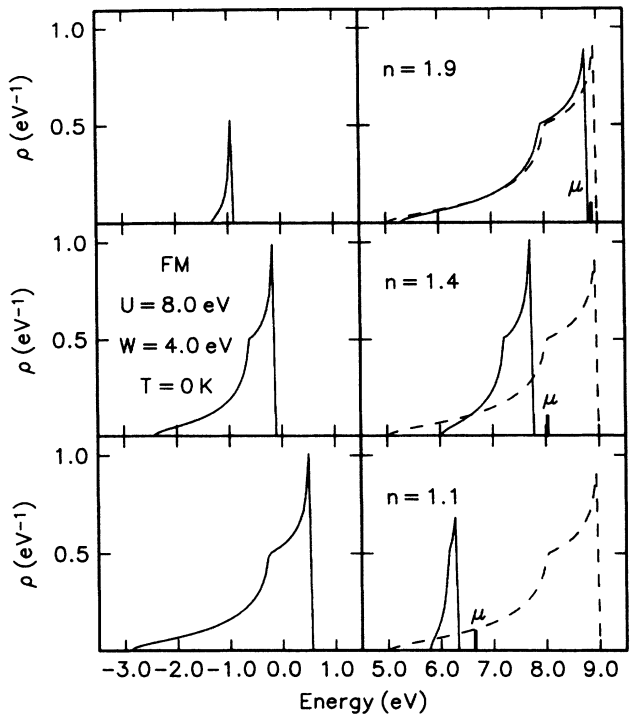

FIG. 4. Quasiparticle density of states for the ferromagnet at $T=0$ K for three different band fillings n. Solid lines belong to $\rho_\uparrow$ and dashed lines to $\rho_\downarrow$. Bars mark the position of the chemical potential μ.

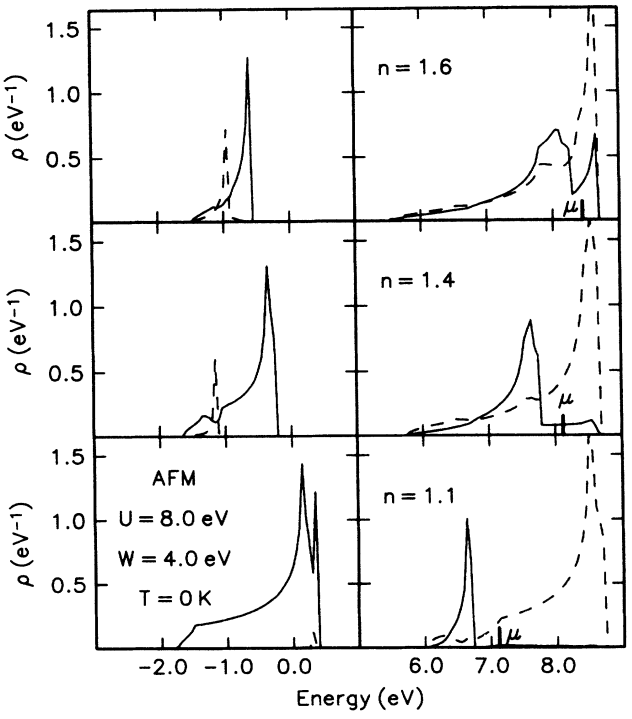

FIG. 5. Quasiparticle density of states for the antiferromagnet at $T=0$ K for three different band fillings n. Solid lines belong to $\rho_{A\uparrow}$ and dashed lines to $\rho_{A\downarrow}=\rho_{B\uparrow}$. Bars mark the position of the chemical potential μ.

energy has been used to sort out the most stable configuration. In a small stripe to the right of the $n=1$ axis the system is antiferromagnetic, while for higher band fillings ferromagnetism becomes stable. This phase diagram exhibits some characteristic deviations from that presented in Ref. 11, which all point to a remarkable structure dependence of the magnetic data of the Hubbard model. The asymmetry of the present phase diagram with respect to the $n=1$ axis is of course a direct consequence of the asymmetric BDOS (Fig. 1). It is, however, worthwhile to mention that the Nagaoka limit[8] for fcc lattices (ferromagnetic ground state for $N_e=N+1$, paramagnetic ground state for $N_e=N-1$) is exactly reproduced by our theory, if we take the limit $U\rightarrow\infty$. With increasing U the antiferromagnetic stripe to the right of the $n=1$ axis becomes smaller and smaller, practically disappearing for $U>100$ eV, and the area of stable ferromagnetic solutions approaches the $n=1$ axis. For $U\rightarrow\infty$ antiferromagnetism is restricted to the half-filled band case, $n<1$ allows only paramagnetism, while for $n>1$ ferromagnetism is stable. Our approach obviously indicates that the Nagaoka theorem is strictly correct excludingly in the $U\rightarrow\infty$ limit and cannot be generalized to finite U.

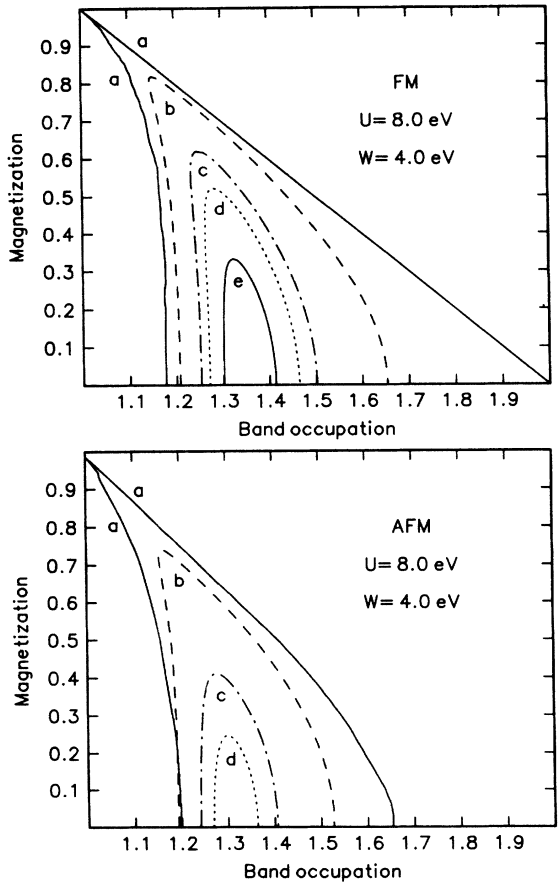

FIG. 6. (Sublattice) Magnetization m as function of band occupation n for the ferromagnet (upper part) and the antiferromagnet (lower part). The lines belong to different temperatures: a, $T=0$ K; b, $T=1500$ K; c, $T=2000$ K; d, $T=2100$ K; and e, $T=2200$ K.

Furthermore, we observe that in an fcc lattice antiferromagnetic solutions exist for a fixed n only if the Coulomb coupling U exceeds a critical value $U_c^{\mathrm{AFM}}(n)$, but contrary to Ref. 11 $U_c^{\mathrm{AFM}}(n)$ remains finite for $n \to 1$. A further striking difference lies in the fact that ferromagnetism is stable up to $n=2$, where the critical Coulomb correlation $U_c^{\mathrm{FM}}(n)$ even decreases to zero for $n \to 2$. The latter is, however, an artifact caused by the singularity of the tight-binding fcc BDOS at the upper band edge (Fig. 1). The simple Stoner criterion for ferromagnetism [$U\rho_o(\mu) > 1$] may give a plausible hint, why for $n \to 2$, i.e., when μ approaches the upper band edge, an arbitrary small U already suffices to favor ferromagnetism. For nondiverging densities of states, however, it is to be expected[11] that ferromagnetism needs a minimum particle as well as a minimum hole concentration, below which ferromagnetism is unstable irrespective of the magnitude of U.

Callaway[17] investigated for the same fcc lattice structure the possibility and stability of ferromagnetic spin waves by evaluating a T-matrix approach of Edwards.[18] The nearest-neighbor hopping $T_1(G)$ is assumed to be positive, so that his BDOS is practically the reflection of our $\rho_0(E)$ in Fig. 1. The somewhat artificial singularity is changed into a finite, but pronounced peak by taking into account the next-nearest-neighbor hopping T_2. The peak appears at the bottom of the band, and consequently ferromagnetism is favored by *low* particle densities n. As to the stability of ferromagnetism the results in Ref. 17 for $n \ll 1$ for which the T matrix procedure should be a reliable approach, are qualitatively very similar to ours for $2-n$ ($n \ll 1$). Antiferromagnetism is not considered in Ref. 17.

To give an illustration we have plotted in Fig. 3 the n dependence of the $T=0$ sublattice magnetization m for $U=8$ eV, i.e., for a rather strongly correlated electron system. In wide regions for the particle density n we find five mathematical solutions for our model, two antiferromagnetic, two ferromagnetic, and one paramagnetic ($m=0$) solution. In cases where two solutions of the same magnetic configuration appear, always that with the higher magnetization turns out to be more stable. In what follows we therefore restrict our considerations excludingly to these solutions. Figure 3 shows also the internal energy $E_0(T=0)=\langle H \rangle / N$ as a function of the band filling n. One gets the usual parabolic behavior, where, except for very small regions, the magnetically ordered phases are lower in energy than the paramagnetic phase. The evaluation of $E_0(T)$-n plots like that in Fig. 3 leads to the magnetic phase diagram in Fig. 2. It is a spe-

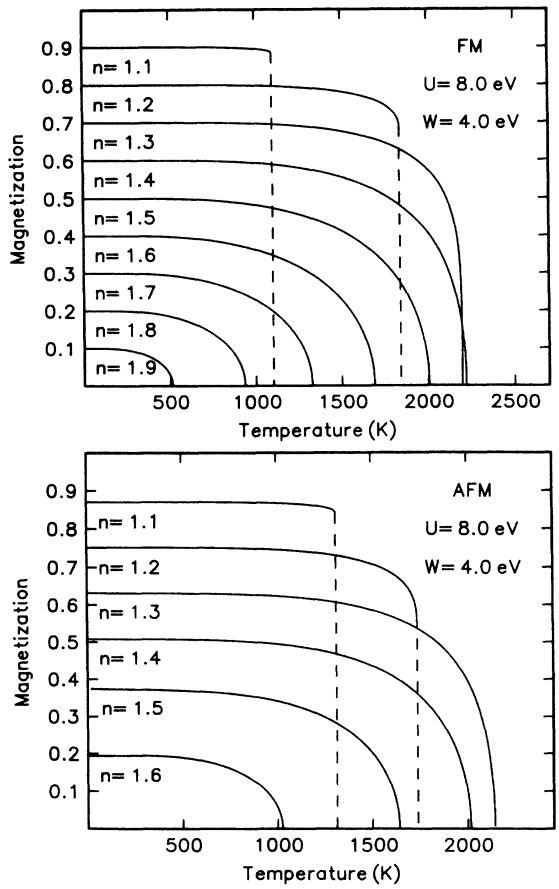

FIG. 7. (Sublattice) Magnetization m of the ferromagnet (upper part) and the antiferromagnet (lower part) as function of temperature T for various band occupations n.

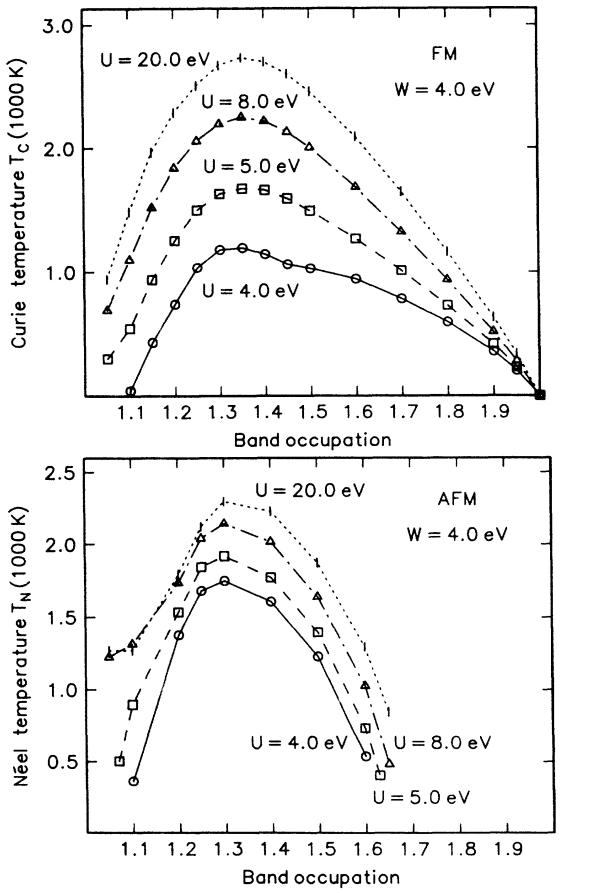

FIG. 8. Curie (Néel) temperature $T_C(T_N)$ for the ferromagnet (upper part) and the antiferromagnet (lower part) as function of band occupation n for various values of the Coulomb coupling U at $W=4$ eV.

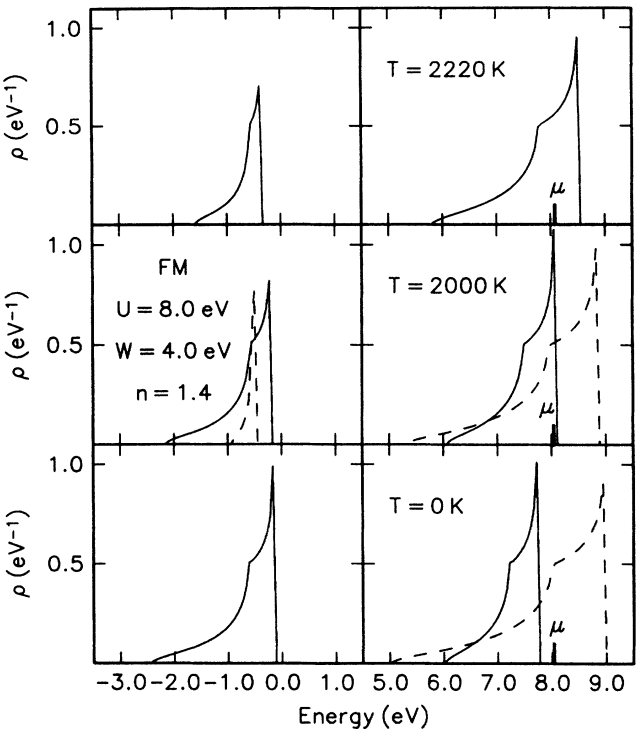

FIG. 9. Ferromagnetic quasiparticle density of states at $n=1.4$ for three different temperatures T. Solid lines belong to $\rho_{\uparrow}$ and dashed lines to $\rho_{\downarrow}$. Bars mark the position of the chemical potential μ.

cial feature that the relevant ferromagnetic $T=0$ solution is always saturated (see Fig. 3). Because of $n>1$ this means $m=2-n$, and is of course again a consequence of the BDOS singularity at the upper band edge.

The magnetic properties of the Hubbard system, as presented so far, find a natural explanation by the respective behavior of the quasiparticle density of states [QDOS, Eq. (23)]. The sublattice QDOS is plotted in Fig. 4 for ferromagnets $[\rho_{A\sigma}(E)=\rho_{B\sigma}(E)=\rho_{\sigma}(E)]$ and in Fig. 5 for antiferromagnets $[\rho_{A\sigma}(E)=\rho_{B-\sigma}(E)=\rho_{\sigma}(E)]$. Both figures show three examples for three different band occupations, in order to illustrate the remarkable influences of electron correlations on the energy spectra. First they split the original Bloch band into a low- and a high-energy Hubbard subband separated by an energy amount of order U. This splitting happens irrespective of the magnetic configuration (paramagnetism, ferromagnetism, or antiferromagnetism). Qualitatively speaking, the low-energy subband refers to an electron hopping over empty sites, while in the high-energy part the electron propagates mainly via lattice points that are already occupied by another electron of opposite spin. The subbands are characterized by spectral weights, which are strongly temperature, carrier-concentration, and possibly even spin dependent. A spectral weight has the physical meaning of a probability quantity being directly given by the area under the respective QDOS curve. It expresses the probability that the itinerant electron will enter an empty or an occupied site, respectively. The weight of the lower (α,σ) subband therefore scales roughly with $(1-\langle n_{\alpha-\sigma}\rangle)$, that of the upper band with $\langle n_{\alpha-\sigma}\rangle$. *Ferromagnetic* saturation in a more than half-filled $(n>1)$ Bloch band means that all holes are from the $\downarrow$ spectrum $(\langle n_{A\uparrow}\rangle=\langle n_{B\uparrow}\rangle=\langle n_{\uparrow}\rangle=1)$. This has the two interesting consequences, that the lower $\downarrow$ subband exhibits vanishing spectral weight and the upper $\downarrow$ subband has ex-

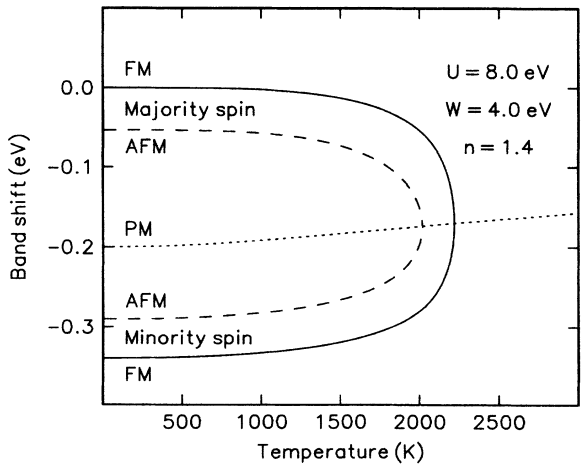

FIG. 10. Band shift $B_{a\sigma}$ as function of temperature T at $n=1.4$. Solid lines indicate the band shift in the ferromagnet, dashed lines belong to the antiferromagnet, and the dotted line is the band shift of the paramagnetic solution.

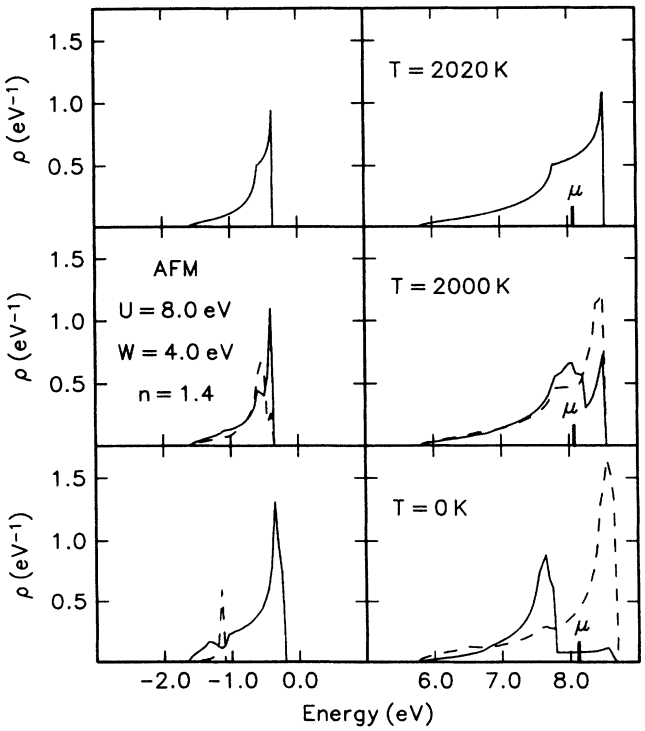

FIG. 11. Antiferromagnetic quasiparticle density of states at $n=1.4$ for three different temperatures T. Solid lines belong to $\rho_{A\uparrow}$ and dashed lines to $\rho_{A\downarrow}=\rho_{B\uparrow}$. Bars mark the position of the chemical potential μ.

actly the nondeformed shape of the free BDOS (Fig. 1). This is clearly to recognize in Fig. 4 for the ferromagnetic $T=0$ QDOS. The chemical potential $\mu(T=0)$ lies always above the upper edge of the upper ↑ subband, guaranteeing therewith $\langle n_{\uparrow} \rangle = 1$.

It is evident from our general theory [see, e.g., Eq. (32)] that the quasiparticle energies [equal to poles of the one-electron Green function (30)] are in the *antiferromagnetic* phase completely spin independent because of the $(A\sigma, B-\sigma)$ symmetry of the self-energy parts. The spectral weights (equal to residues of the Green-function poles), however, are spin-dependent. That means that ↑ and ↓ spectra in a sublattice QDOS occupy exactly the same energy region, but with different spectral weights. The latter is responsible for the nonzero sublattice magnetization, the first for the fact that the antiferromagnet never reaches saturation (see Figs. 3 and 5). While ferromagnetism is mainly due to a spin-dependent shift of the quasiparticle subbands, antiferromagnetism results from spin-dependent state densities without any exchange shift of the spin spectra. This conclusion is in complete agreement with that given in Ref. 11. There is, however, an interesting difference concerning the antiferromagnetic phase. For the simple BDOS, used in Ref. 11, the QDOS exhibits in each subband an additional splitting. The so-called Slater gap is a consequence of the magnetic Brillouin zone being only half the chemical Brillouin zone. For the antiferromagnetic (MnO-type) structure, and the BDOS of Fig. 1, the Slater gap obviously opens for different **k** directions in different energy regions, so that the total QDOS does not show a Slater gap (Fig. 5).

Let us now discuss the finite temperature effects. Figure 6 shows examples of the n dependence of the ferromagnetic and antiferromagnetic sublattice magnetization m for different temperatures. We observe that the curves for the two magnetic solutions move together narrowing therewith the band-filling region, in which band ferromagnetism or antiferromagnetism is possible. This region becomes smaller with increasing temperature pointing to an electron concentration of about 1.35. The temperature dependence of the sublattice magnetization (Fig. 7) is Brillouin-function-like when n exceeds a U-dependent critical value n_s. This behavior, normally ascribed to a Heisenberg ferromagnet of localized magnetic moments, leads to phase transitions of second order at $T_{C,N}$. For band fillings closer to $n=1$ $(1 \leq n \leq n_s)$ the magnetic-nonmagnetic phase transition becomes discontinuous. Similar observations have been reported in Ref. 11. The existence of first-order as well as second-order phase transitions seems to be an inherent property of the Hubbard model.

The temperature, at which the spontaneous (sublattice)

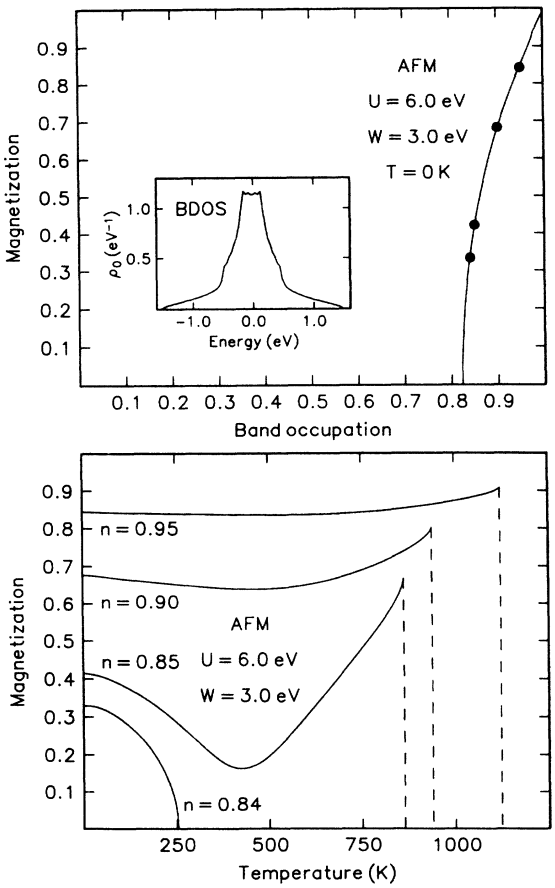

FIG. 12. Sublattice magnetization m as function of band occupation n (upper part) and as function of temperature T (lower part) for the antiferromagnet. The corresponding BDOS is plotted as an inset.

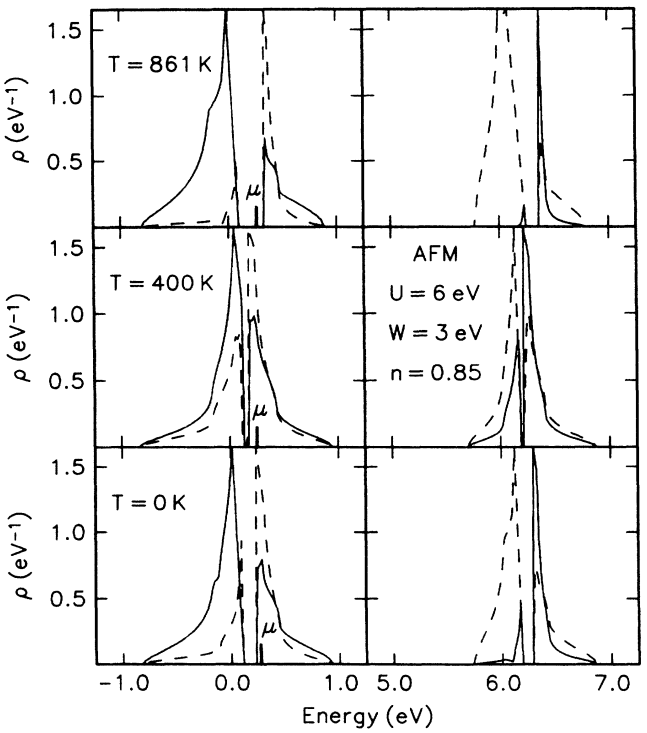

FIG. 13. Antiferromagnetic quasiparticle density of states at $n=0.85$ for three different temperatures T. Solid lines belong to $\rho_{A\uparrow}$ and dashed lines to $\rho_{A\downarrow}=\rho_{B\uparrow}$. Bars mark the position of the chemical potential μ. The corresponding BDOS is shown in Fig. 12.

magnetization disappears, defines the (Néel) Curie temperature, which turns out to be strongly dependent on the Coulomb coupling U and the particle density n. Figure 8 shows that for a fixed U the Curie temperature T_C runs as function of n through a maximum at about $n=1.35$. As can be read off from the phase diagram in Fig. 2, the system needs a minimum occupation n in order to become ferromagnetic or antiferromagnetic. This minimum occupation is U dependent, approaching 1 for $U\rightarrow\infty$ and 2 for $U\rightarrow 0$. As already explained, the latter is a consequence of the singular behavior of the BDOS at the upper band edge (Fig. 1). The maximum of the T_N-n curve in Fig. 8 occurs also very close to $n=1.35$, but generally the region where antiferromagnetic solutions exist is smaller. Note that in Fig. 8 the critical temperatures are plotted as functions of n for various U irrespective of whether or not the considered magnetic configuration is really the most stable one. One has to combine Fig. 8 with Fig. 2. In any case the critical temperatures increase monotonically with increasing U, reaching finally, however, a saturation value. Contrary to the simpler Stoner model, the $T_{C,N}$ values are of realistic orders of magnitude for all parameter-sets. This is a direct consequence of the temperature behavior of the QDOS. In the ferromagnetic Stoner model the thermal energy of order $k_B T_C$ has to bridge a shift of order U between the $\sigma=\uparrow$ and $\sigma=\downarrow$ spin bands:

$$k_B T_C^{Stoner}\approx Um \tag{40}$$

For $U=8$ eV and $m=0.63$ this means a T_C^{Stoner} of about 6×10^4 K. In our theory, however, only the spin splitting of the two Hubbard bands has to be removed, while the Hubbard gap (of order U) persists to temperatures above T_C (see Fig. 9). The spin splitting of the two subbands is excludingly due to the spin-dependent band shift $B_{\alpha\sigma}$, which is of course α independent for ferromagnets. As an example we have plotted $B_\uparrow$ and $B_\downarrow$ in Fig. 10 for $U=8.0$ eV, $W=4.0$ eV, $n=1.4$ as functions of temperature. One may roughly estimate as an upper boundary

$$T_C\approx\frac{1}{k_B}|B_\uparrow(T=0)-B_\downarrow(T=0)|$$
$$\approx\frac{1}{k_B}0.35\text{ eV}\approx 4200\text{ K}\,, \tag{41}$$

which is at least one order of magnitude smaller than the Stoner value. As already discussed in detail, the antiferromagnetic sublattice QDOS does not exhibit an exchange splitting in the usual sense. Majority (minority) spins are produced by different $\uparrow$- and $\downarrow$-state densities, where the difference decreases when T approaches T_N (see Fig. 11). In this case $B_{\alpha\sigma}$ cannot be interpreted as a direct shift of the center of gravity of any subband. Antiferromagnetic quasiparticle energies contain both terms $B_{A\sigma}$ and $B_{B\sigma}=B_{A-\sigma}$. The spectral weights, however, depend either on $B_{A\sigma}$ or $B_{B\sigma}$, therewith producing the antiferromagnetic ordering. This can be read off already from the formal solution (30) for the one-electron Green function.

Let us finally comment on an interesting feature, born out of Ref. 11, which is called "heat magnetization." This denotes the phenomenon that the sublattice-magnetization of an antiferromagnet with increasing temperature in certain temperature regions. We think that this pecularity is connected with the opening of a Slater gap for $T<T_N$. For our MnO-type antiferromagnet we do not observe such a heat magnetization, probably because we found no Slater gap. To demonstrate the phenomenon we have solved our system of equations for the same symmetric model BDOS, which has been used in Ref. 11. The BDOS is plotted as inset in Fig. 12. A self-consistent antiferromagnetic solution for the sublattice magnetization m appears for $n>0.82$. The m versus n plot is now symmetric to the $n=1$ axis because of particle-hole symmetry. For four values of the band occupation n, marked by solid dots in Fig. 12, we have calculated the temperature dependence of m (Fig. 12). We observe regular behavior with a second-order transition for $n=0.84$, but a drastic heat-magnetization for $n\geq 0.85$ with an abrupt breakdown of the spontaneous magnetic order at T_N. The temperature behavior of the QDOS, plotted in Fig. 13 for $n=0.85$, illustrates the underlying mechanism. For low temperatures the chemical potential μ lies in a region of high minority-spin density of states (DOS). With increasing temperature the corresponding subband shifts to higher energy, so that μ changes into regions of less minority-spin DOS. This means of course a higher magnetization with increasing temperature, being especially drastic when μ enters the Slater gap. This gives evidence that the heat magnetization is not an artifact of the theoretical approach, but most probably an inherent property of the s-band Hubbard model. The appearance of heat magnetization in the antiferromagnetic phase in Ref. 11 turns out to be caused by special features of the antiferromagnetic lattice structure.

V. SUMMARY

We have used the s-band Hubbard model to investigate the possibility of magnetic order in narrow nondegenerate energy bands. To study the stability of different magnetic configurations we started from a realistic rock-salt structure with a two-sublattices decomposition of the frequently realized MnO type. We used an effective-medium approach for an approximate, but self-consistent solution of the underlying many-body problem.

Ferromagnetic as well as antiferromagnetic solutions appear for more than half-filled bands and for Coulomb interactions U, which exceed an n-dependent critical value $U_c(n)$. Decisive for spontaneous magnetic order are certain higher equal-time correlation functions of type $\langle c_{i-\sigma}^\dagger c_{j-\sigma} n_{i\sigma}\rangle$, which give rise to a spin-dependent subband shift in the ferromagnetic quasiparticle density of states or to spin-dependent state densities of the energy spectra in an antiferromagnetic system. Such higher correlation terms do not appear in Hubbard I or coherent potential approximation (CPA) treatments of the Hubbard model. Our finite-temperature results predict an optimum band filling of $n\approx 1.35$ for the critical tempera-

tures T_C and T_N. These transition temperatures appear for all parameter constellations (U,n) in realistic orders of magnitude. They increase as a function of the Coulomb coupling U, tending, however, to saturation for $U \rightarrow \infty$.

ACKNOWLEDGMENTS

Financial support of the Deutsche Forschungsgemeinschaft (Sonderforschungsbereich 225) is gratefully acknowledged.

[1]J. Hubbard, Proc. R. Soc. London **A276**, 238 (1963).
[2]J. Hubbard, Proc. R. Soc. London **A277**, 237 (1964).
[3]J. Hubbard, Proc. R. Soc. London **A281**, 401 (1964).
[4]E. H. Lieb and F. Y. Wu, Phys. Rev. Lett. **20**, 1445 (1968).
[5]G. Beni, T. Holstein, and P. Pincus, Phys. Rev. B. **8**, 312 (1973).
[6]J. E. Hirsch, Phys. Rev. B **35**, 1851 (1987).
[7]J. Callaway, D. P. Chen, and R. Tang, Phys. Rev. B **35**, 3705 (1987).
[8]Y. Nagaoka, Phys. Rev. **147**, 392 (1966).
[9]J. Kanamori, Prog. Theor. Phys. (Kyoto) **30**, 275 (1963).
[10]P. W. Anderson, in *Solid State Physics*, edited by F. Seitz, D. Turnbull, and H. Ehrenreich (Academic, New York, 1963), Vol. 14, p. 99.
[11]W. Nolting and W. Borgiel, Phys. Rev. B **39**, 6962 (1989).
[12]K. Terakura, T. Oguchi, A. R. Williams, and J. Kübler, Phys. Rev. B **30**, 4734 (1984).
[13]J. Kübler and A. R. Williams, J. Magn. Magn. Mater. **54-57**, 603 (1986).
[14]W. Nolting, W. Borgiel, V. Dose, and Th. Fauster, Phys. Rev. B **40**, 5015 (1989).
[15]W. Borgiel and W. Nolting, Z. Phys. B **78**, 241 (1990).
[16]W. Nolting, J. Braun, G. Borstel, and W. Borgiel, Phys. Scr. **41**, 601 (1990).
[17]J. Callaway, Phys. Rev. **170**, 576 (1968).
[18]D. M. Edwards, J. Appl. Phys. **39**, 481 (1968).